Heliyon 10 (2024) e33137

Contents lists available at ScienceDirect

Heliyon

journal homepage: www.cell.com/heliyon

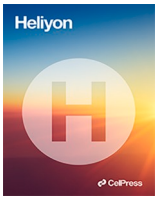

Research article

Common carp sperm chromatin as an economical and effective remover for benzo(*a*)pyrene from pollutants

Zhikang Jiang, Junsheng Li *, Guoxia Huang, Liujuan Yan, Ji Ma

School of Biological and Chemical Engineering, Guangxi University of Science and Technology, Wenchang Road 2, Liuzhou, 545006, Guangxi, China

ARTICLE INFO

Keywords:
Chromatin
PAHs
benzo(*a*)pyrene
Removal
Economical
Effective

ABSTRACT

Benzo (a) pyrene is a highly carcinogenic polycyclic aromatic compound, difficult to be degraded, widely present in the environment. However, there is currently no cost-effective and efficient method for removing benzo (a) pyrene. In this study, a feasible method was introduced to cheaply and efficiently adsorb benzo(*a*)pyrene using chromatin. Scanning electron microscopy analysis showed that the chromatin had a filamentary fiber structure. Fourier transform infrared (FTIR) spectroscopy showed that benzo(*a*)pyrene formed a bond with the chromatin. Effective binding was confirmed using fluorescence microscopy. Influence factors exploration experiments indicated that the amount of benzo(*a*)pyrene adsorbed by chromatin was 0.16 mg g^{-1}. The adsorption process of BaP by chromatin is consistent with a pseudo-second-order kinetics model of adsorption. The adsorption isotherm model is consistent with the langmuir isotherm model.This study suggests that chromatin can be utilized as a ordinary and high efficiency adsorbent for removing benzo(*a*)pyrene and can be utilized in further studies.

1. Introduction

Polycyclic aromatic hydrocarbons (PAHs) are the chemical compounds formed by combining several benzene rings in different arrangements [1]. They originate mainly from the incomplete combustion of fossil energy sources in industrial production [2]. The stable structure of PAHs makes them difficult to degrade in the environment, and they are prone to accumulation, causing serious harm to the environment and living organisms [3]. In the 1980s, the U.S. Environmental Protection Agency listed 16 PAHs as priority control pollutants [1]. The most notable characteristics of PAHs are carcinogenicity, teratogenicity and mutagenicity [4]. Benzo(*a*)pyrene (BaP) is a strong carcinogen among polycyclic aromatic hydrocarbons, which is recognized as one of the three major carcinogens in the world, and the World Health Organization (WHO) has classified BaP as a Group I carcinogen [4]. Incomplete combustion of organic substances can produce the polycyclic aromatic hydrocarbon BaP, which consists of five benzene rings attached to each other, and widely exists in the tailpipe of automobile emission, fried food, asphalt and smoke [5]. In studies of BaP, it has been found to cause a number of major diseases such as leukaemia and liver cancer [6]. In recent years, many methods such as adsorption [7], biodegradation [8], advanced oxidation [9], ultrasonic degradation [10], and bioremediation [11] have been attempted for BaP removal. All of these methods are flawed to some degree. In particular, the adsorption method offers the advantages of simplicity of operation, cost-effectiveness, high removal capacity, and no other toxic degradation in use, which makes it an excellent method for treating

* Corresponding author.
E-mail addresses: 1848541190@qq.com (Z. Jiang), junshenglee63@aliyun.com (J. Li), 251493952@qq.com (G. Huang), 274187443@qq.com (L. Yan), 93829237@qq.com (J. Ma).

https://doi.org/10.1016/j.heliyon.2024.e33137
Received 10 January 2024; Received in revised form 13 June 2024; Accepted 14 June 2024
Available online 14 June 2024

pollutants [12]. Conventional adsorption method is to remove the pollutants by soil, activated carbon or some biomass materials.BaP belongs to organic molecules and forms co-adsorbents with surfactants and metal ions and other substances, which will lead to a decrease in adsorption capacity. In addition, the adsorbents are susceptible to degradation, leading to poor treatment results. Therefore, this study investigates the feasibility of chromatin as an adsorbent for treating BaP fouling based on the mechanism of DNA and planar polycyclic substance insertion binding.

DNA has an important role in the various functional applications of living organisms and is a genetic material that primarily carries genetic information. DNA has also been the target of exogenous attacks and biological damage. In 1961, Lerman discovered that some molecules with planar aromatic ring structures could intercalate into base pairs, and these small molecules were called DNA insertion agent molecules [4,13]. Based on this model, it has been shown that anthraquinones, acridines and naphthylimides are able to intercalate into the base pairs of DNA by intercalating bite to achieve intercalation in vitro. The above studies provide a possibility for the removal of PAHs by DNA-rich substances [14,15]. DNA has been proposed as an adsorbent for the removal of BaP, but this method relies on the separation of DNA and solution by magnetic beads, which increases the cost and operational difficulties of using adsorbents during the adsorption process [4]. Therefore, it is necessary to explore a cost-effective and efficient adsorbent enriched with DNA for removing BaP from pollutants.

The main components of chromatin are DNA and proteins. The linear structure with nucleosome as the basic unit contains about 50bp of connecting DNA linked together, and the nucleosome is assembled by histone proteins with 1.75 circles of 146bp of DNA wrapped around the periphery [16]. Thus chromatin not only possesses some of the properties associated with DNA, but also is a huge bio-macromolecular substance that naturally stabilizes and fixes DNA. Chromatin is widely found in the spermathecae of male organisms from a wide range of sources and is expected to be an inexpensive adsorbent. In this study, we propose to use the globally widely available carp sperm nests as raw material for extracting carp sperm chromatin, and use carp sperm chromatin as a substitute of DNA to capture and remove BaP.

In the present research paper, we propose chromatin, a novel adsorbent for removal of BaP, to reduce the operational cost of using magnetic beads to separate DNA first. The main purpose of this article is to further expand the use of DNA or chromatin for economical and effective removal of polycyclic aromatic hydrocarbons (PAH) pollutants based their intercalations with DNA or chromatin. Therefore, we characterized the carp sperm chromatin properties before and after adsorption of BaP using fluorescence microscopy, SEM, and FTIR. We also investigated various factors that might affect the adsorption performance of carp sperm chromatin on BaP, includes BaP solution pH, reaction temperature, time of reaction, chromatin dose and initial BaP solution concentration. In addition, we also utilized kinetic and thermodynamic methods to analyze the process of carp sperm chromatin adsorbing BaP.

2. Materials and methods

2.1. Experimental drugs and information

BaP (Dr. Ehrenstoff GmbH, Augsburg, Germany, standard) was dissolved in ethanol (Chengdu Cologne Chemical Co., Ltd., China, 98 %) and diluted with Tris-HCl buffer solution (pH 7.4) to make a stock solution (Tris: Shanghai Yuanye Biotechnology Co., Ltd., China, analytically pure, 99.5 %. HCl: Xilong Science Co.). Chromatin was prepared according to the Artman method using spermatophores of Asian male carp purchased from the market and stored at −70 °C. The chromatin was extracted from the spermatophores of Asian male carp by the Artman method. Sodium chloride, trisodium citrate, and sucrose used in the chromatin extraction process were produced by Xilong Scientific Co, 99 %. The configuration solutions in the experimental studies were refrigerated at 4 °C in a refrigerator. The pH value of the solutions was adjusted with Tris-HCl buffer solution.

2.2. Instrumentation

A thermostatically controlled water bath of type HH-4, manufactured in China, was used for the temperature in the experimental reaction of benzo(*a*)pyrene. All centrifugation operations in the experimental study were performed using a cryogenic centrifuge manufactured by Sigma, Germany. The homemade chromatin was freeze-dried using an alpha1-4LD + machine from Christ, Germany. BaP concentrations were converted by using a Cary Eclipse fluorescence spectrophotometer (Agilent Technologies, USA). Chromatin was examined before and after the adsorption experiments using an American model Thermo Scientific Nicolet is 10 FTIR spectrometer. DM4B fluorescence microscope (Leica, Germany) was used for fluorescence observation of chromatin and chromatin after adsorption of BaP. Scanning electron microscope (Czech Republic TESCAN MIRA LMS).

2.3. Chromatin preparation

Chromatin was extracted following the method proposed by Artman [17]. A 1.5 % solution of $C_6H_5Na_3O_7$ was used in the ratio of 1:10 by mass to carp testicles and then homogenised in a homogeniser. Take the precipitate saved by centrifugation in a centrifuge using 12000 rpm for 15 min. Subsequently, the precipitate after centrifugation was taken and added to the precipitate in the ratio of 1:10 by mass of 0.25 M sucrose-1.5 % sodium citrate solution and homogenised using a homogeniser and centrifuged to obtain the precipitate. Sperm cells were prepared by adding 0.88 M sucrose-1.5 % sodium citrate solution to the precipitate in the ratio of 1:30 by mass, mixing well and standing for 10 min. The rested solution was taken and processed in a centrifuge at 12,000 rpm for 15 min. The precipitate after centrifugation was taken and the resulting precipitate was washed three times with a solution at a concentration of 0.05 M Tris HCl - 0.15 M NaCl (pH 7.5) at a mass ratio of 1:5 to obtain a purer cell nucleus. A 0.01 M Tris-HCl (pH 8.0) solution was

added to the washed precipitate at a mass ratio of 1:10 and further processed using a homogeniser. Finally, chromatin was obtained by centrifugation at 12,000 rpm for 15 min and the resulting precipitate was processed using a freeze dryer.

2.4. Adsorption experiment

To investigate the effect of reaction time on the removal of BaP by chromatin, the pH of the working solution was set at 7.4, the chromatin dose was 1.5 g L^{-1}, the volume of BaP working solution was 4 mL, and the initial concentration of the solution was 100 μg·L^{-1}, 150 μg·L^{-1}, 200 μg·L^{-1}, 250 μg·L^{-1}, and 300 μg·L^{-1}, respectively.The supernatant of the BaP working solution was measured in a water bath after After reaction for 20, 40, 60, 80, 100, 120, 140, 160, and 180 min, the absorbance values of the supernatants were measured to find the appropriate reaction time.

To investigate the effect of temperature on the removal of BaP by chromatin, pH was set 7.4, six treatments of temperature heating were set at 25 °C, 30 °C, 35 °C, 40 °C, 45 °C, 50 °C, and 4 mL of BaP solution with concentrations of 100 μg·L^{-1}, 150 μg·L^{-1}, 200 μg·L^{-1}, 250 μg·L^{-1}, 300 μg·L^{-1}, respectively, were added to a solution of 1.5 g L^{-1} chromatin. The absorbance value of its supernatant was measured after 140 min of shaking bed reaction to find the suitable temperature of adsorption reaction.

In order to study the effect of solution pH on the BaP removal rate, the pH of the working solution was set at 6.4, 7, 7.4, 8,9, the chromatin dose was 1.5 g L^{-1}, the volume of the BaP working solution was 4 mL, and the initial concentration of the solution was 200ug·L^{-1}. The absorbance value of the supernatant was measured after the reaction was carried out for 140 min in a water bath to study the effect of solution pH on the BaP removal rate.

In order to find out the appropriate amount of chromatin, 0.5 g L^{-1}, 1 g L^{-1}, 1.5 g L^{-1}, and 2 g L^{-1} of chromatin were added to 12 portions of 4 mL of BaP solution with concentrations of 100 μg·L^{-1}, 200 μg·L^{-1}, and 300 μg·L^{-1}, respectively, and the shaking bed reaction was carried out for 140 min.

In order to investigate the effect of BaP solution concentration on the adsorption performance of chromatin, 100 μg·L^{-1}, 150 μg·L^{-1}, 200 μg·L^{-1}, 250 μg·L^{-1}, and 300 μg·L^{-1} BaP solutions were used as the solutions to be adsorbed, and adsorbent dosage of 1.5 g L^{-1}, pH = 7.4, and the shaker reaction was carried out for 140 min.

The fluorescence intensity value of the solution at the end of the reaction was determined using a fluorescence spectrophotometer. The concentration of BaP in the solution was calculated using the fluorescence intensity values. The parameters of the fluorescence spectrophotometer were as follows: excitation wavelength 385 nm, scanning range 400–600 nm, scanning speed Fast, voltage 600, slit: $E_x = 5$ nm, $E_m = 5$ nm, fluorescence emission peaks at 406 nm, 430 nm, and 456 nm, respectively. The absorption peak at 430 nm was chosen as the data for linear equation calculation. The removal rate (R, %) and adsorption capacity (q_e, mg·g^{-1}) of BaP were calculated according to the following equation:

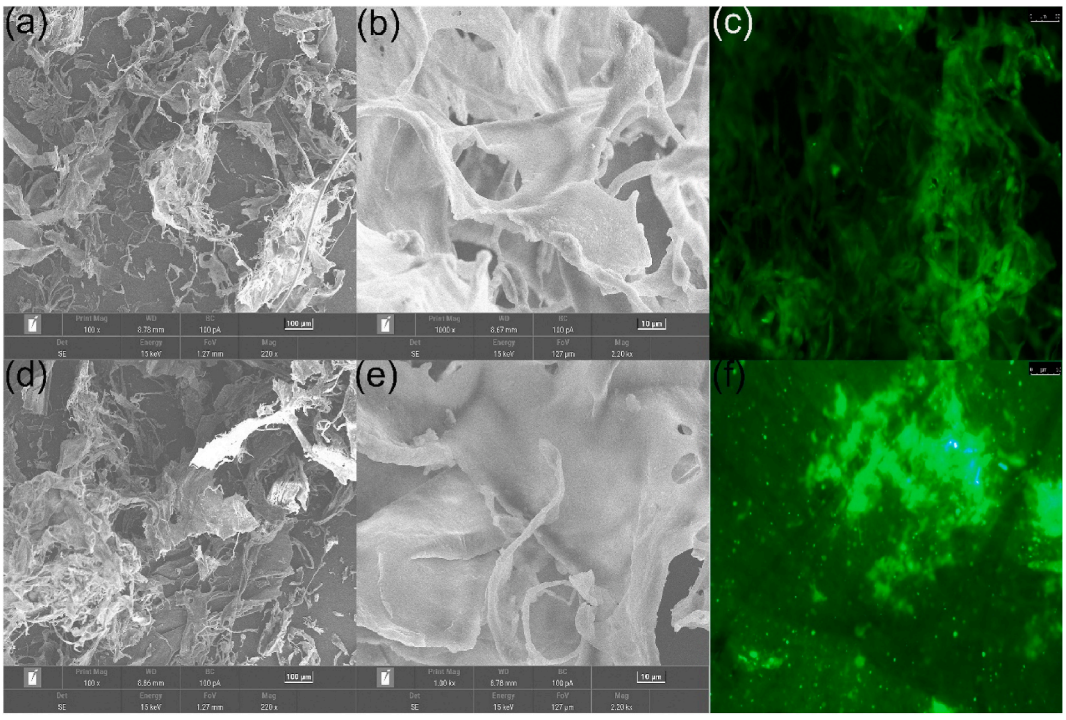

Fig. 1. (a) and (b) Scanning electron micrograph of chromatin before adsorption, (d) and (e) Scanning electron micrograph after chromatin adsorption, (c) Fluorescence microscope image before chromatin adsorption, (f) Fluorescence microscope image after chromatin adsorption.

$$R(\%) = \frac{C_0\text{-}C_e}{C_0} \times 100\%$$

$$q_e = \frac{(C_0\text{-}C_e)V}{W}$$

where C_0 (ug·L^{-1}) represents the concentration of BaP solution in the absence of reaction, Ce (ug·L^{-1}) represents the concentration of BaP solution at the end of the reaction, V (mL) represents the volume of BaP solution, and W (mg) represents the mass of chromatin.

3. Analysis of experimental results

3.1. SEM and fluorescence microscope observation analyses

The scanning electron micrographs and fluorescence diagrams before and after the adsorption of BaP by chromatin are demonstrated in Fig. 1. As shown in Fig. 1a,b,d,e, from the scanning electron micrographs before and after the adsorption of BaP by chromatin, it can be found that there are some filamentary fiber structures in the chromatin, which increases the contact area between the adsorbent and the BaP molecules to a certain extent, and facilitates the adsorption process. As shown in Fig. 1c–f, the fluorescence microscopy observation shows that there is a significant change in the fluorescence intensity of chromatin before and after adsorption of BaP, which is related to the strong fluorescence emitted by planar macromolecules such as BaP themselves, because DNA in chromatin does not emit fluorescence, while proteins in it emit weak fluorescence. By comparing the SEM and fluorescence microscope observations before and after chromatin adsorption of BaP, it can be confirmed that chromatin has a strong adsorption capacity for BaP.

3.2. FTIR analyses

As shown in Fig. 2, in order to better show the changes in FTIR absorption peaks before and after adsorbent adsorption, the FTIR spectrum in this study is presented in two wavelength ranges of 400–1300 cm^{-1} and 100-3000 cm^{-1}. Compared with the infrared absorption peaks of chromatin before adsorption of BaP, it could be found from the results of Fig. 2a and c that the absorption peaks of the chromatin infrared spectrum after adsorption of BaP showed more new peaks in the range of 400–800 cm^{-1}, which should originate from the BaP absorption of adsorbent molecules. It was reported that some vibrational peaks in the range of 400–1300 cm^{-1} were characteristic peaks representing sugars, phospholipids, and DNA skeletons in DNA molecules. For example, 833 cm^{-1} represented sugar-phospholipid strand vibrations, 894 cm^{-1} represented deoxyribose vibrations, 966 cm^{-1} represented DNA backbone labeling, 1055 cm^{-1} represented sugar-phospholipid salt vibrations, 1087 cm^{-1} represented phosphate symmetrical stretching bands, and 1228 cm^{-1} represented phosphate misalignment peaks [18–21]. All of the above characteristic peaks concerning the sugar and phosphate structures in DNA also appeared in the spectrum of Fig. 2c. Correlation studies have shown that the infrared absorption peaks appearing at 455 cm^{-1}, 494 cm^{-1}, 534 cm^{-1}, 634 cm^{-1}, and 668 cm^{-1} in Fig. 2c originated from the bending of γ (C–H) in BaP,

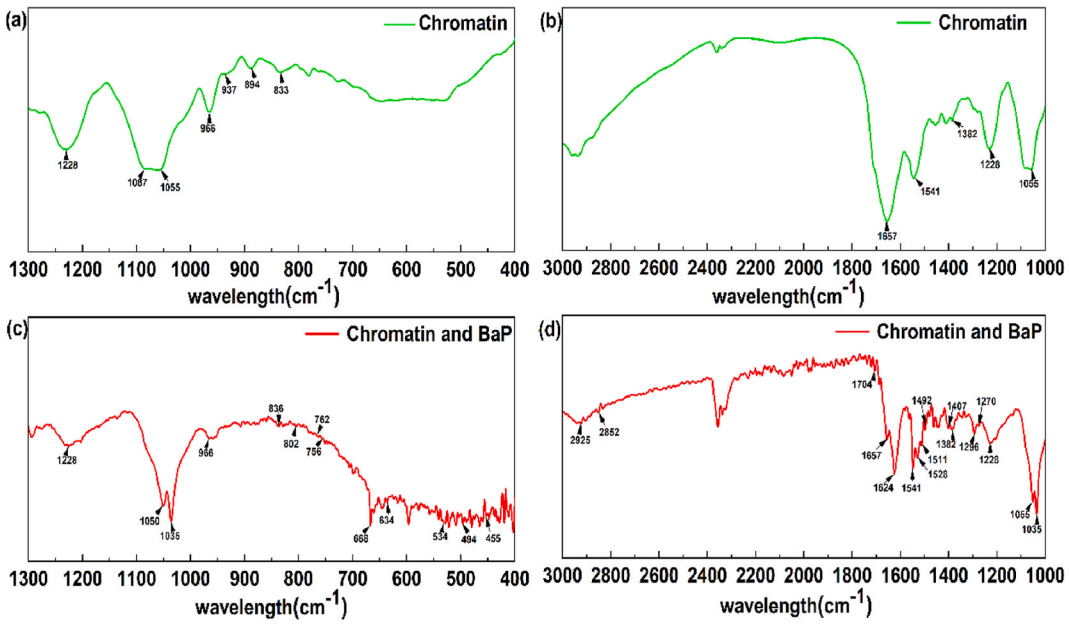

Fig. 2. (a) and (b) Chromatin infrared map, (c) and (d) Infrared image after chromatin adsorption of BaP.

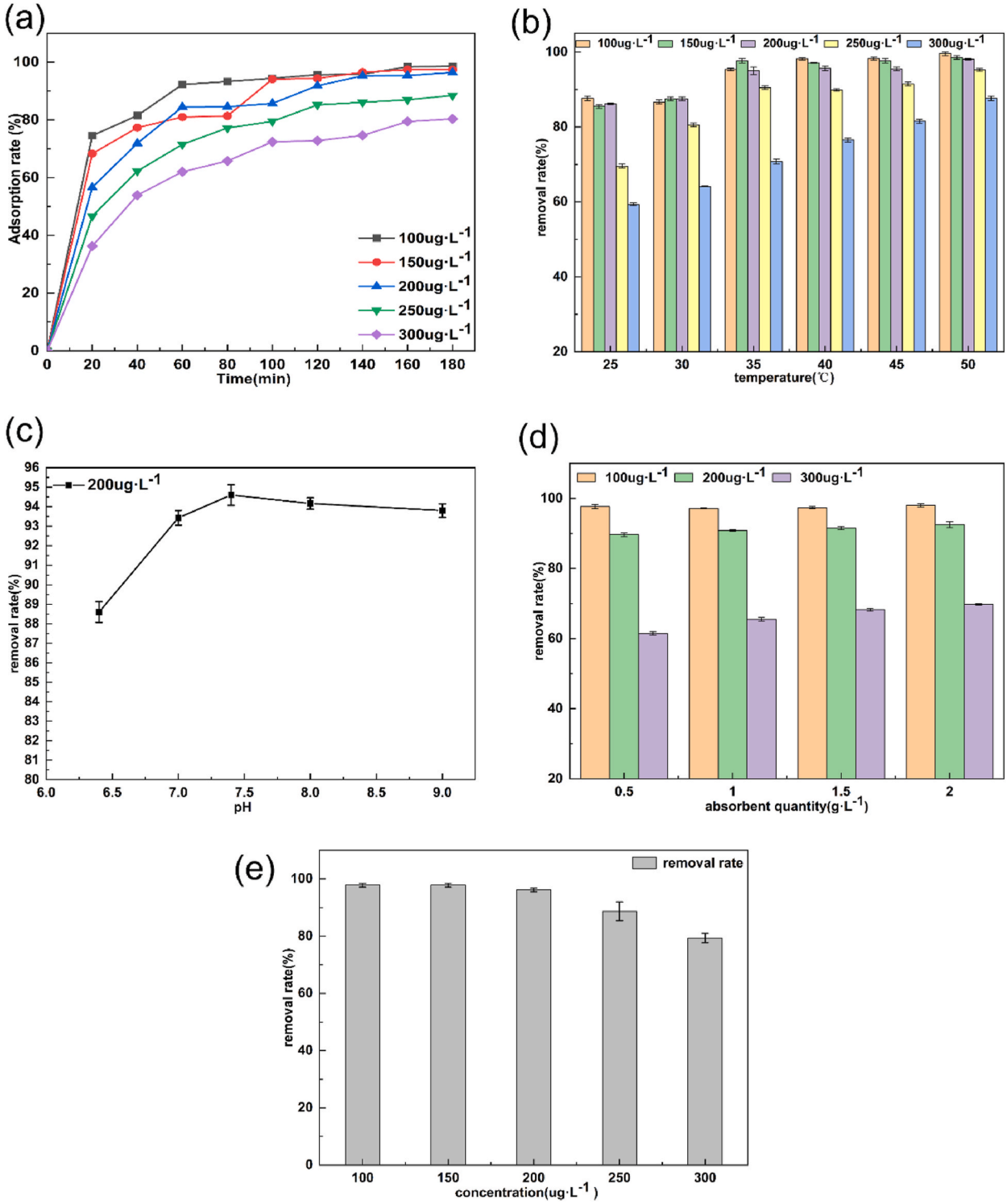

Fig. 3. (a) The effect of reaction time on the efficiency of BaP removal by chromatin. (b) The effect of reaction temperature on the efficiency of BaP removal by chromatin. (c) The effect of pH of BaP solution on the efficiency of chromatin removal (d) The effect of chromatin quality on the removal efficiency of BaP. (e) The effect of initial concentration of BaP solution on the efficiency of chromatin removal.

while the new peaks appearing at 756 cm^{-1}, 762 cm^{-1}, and 802 cm^{-1} were due to the twisting of the τ (C–C) ring in BaP [22]. As shown in Fig. 2b and d, the FTIR spectra of chromatin before and after adsorption also changed more in the range of 1000–2000 cm^{-1}. The A-T and C-G base pair vibrational peaks specific to double-stranded DNA were shown at 1540 cm^{-1} in Fig. 2b, and the infrared absorption peak specific to protein carbonyls in chromatin appeared at 1657 cm^{-1} [16]. Comparing Fig. 2d and b, new FTIR absorption peaks appear at 1270 cm^{-1}, 1296 cm^{-1}, 1407 cm^{-1}, 1492 cm^{-1}, 1511 cm^{-1}, 1528 cm^{-1}, 1624 cm^{-1}, 2852 cm^{-1}, and 2925 cm^{-1}. It was reported that the FTIR absorption peaks at these positions were related to the stretching vibration and δ (C–H) vibration of the ring in the BaP molecule [22]. By comparison of the characteristic peaks associated with the FTIR spectra, it can be confirmed that chromatin forms an effective binding to the BaP molecule.

3.3. The effect of reaction time on the efficiency of BaP removal by chromatin

In the reaction of BaP removal by chromatin, the length of reaction time is an important factor affecting the efficiency of substance adsorption. A suitable reaction time helps to improve the utilisation of chromatin. It could be found from the results of Fig. 3a that the adsorption rates first increases and then gradually leveled off with the increase of adsorption time. When the adsorption time was gradually increased from 20 min to 140 min, the increase in the adsorption rate at each treatment was more than 35 %, and the increase in the adsorption rate was smaller when the adsorption time continued to be extended. This may be due to the limited number of adsorption sites provided by the adsorbent when the mass of chromatin is certain. In the beginning of the process of chromatin removal of BaP, there were sufficient adsorption sites on chromatin for BaP to be adsorbed rapidly. As the reaction time increases, the number of adsorption sites on chromatin decreases, which is not conducive to the continuation of adsorption, so the adsorption rate stabilizes. Therefore, from the consideration of adsorption efficiency, saving time and cost, 140 min should be the optimal adsorption time.

3.4. The effect of reaction temperature on the efficiency of BaP removal by chromatin

As showed in Fig. 3b, when the temperature gradually increased, the removal rate was the first to maintain a large rate of increase, and then leveled off. As the reaction temperature increases from 25 °C to 35 °C at 5 °C intervals, the BaP removal rate of chromatin increased at least 10 % for all BaP solutions. As the reaction temperature increases from 35 °C to 50 °C at 5 °C intervals, only in the 300 $\mu g \cdot L^{-1}$ BaP solution, the BaP removal rate of chromatin gradually increased, while the BaP removal rates of chromatin for the other four concentrations of BaP solutions gradually decreased and/or tended to equilibrium. This phenomenon may be due to the fact that the structure of chromatin in the solution gradually changed from compact to loose with the gradual increase of temperature, exposing more adsorption sites to bind with BaP molecules in the solution, which improved the BaP removal rate. The DNA and protein in chromatin are mainly entangled together by hydrogen bonding, and the histones that play a role in fixation are tightly held together by this force, and with the increase of temperature, the possibility is provided for the disappearance of this force [16,23,24]. Therefore, the BaP removal rate increases with increasing temperature. But when the concentration of the liquid increases, more BaP molecules interact with the chromatin, which suggests that the removal rate gradually increases with increasing temperature at higher concentrations. On the contrary, When the BaP solution is more concentrated, although its BaP removal rate gradually increases with the increase of temperature, many BaP molecules cannot interact with chromatin, resulting in lower levels of BaP removal rate.

3.5. The effect of pH of BaP solution on the efficiency of chromatin removal

From Fig. 3c, it can be found that the change of pH has some influence on the adsorption effect, and the removal rate of BaP by chromatin took the lead in gradual increase and then decrease. The best removal rate was 94 % at pH of 7.4. When the pH was less than 7.4, the removal rate decreased, which may be due to the amino acids of DNA was gradually positively charged, and the electrostatic interaction between chromatin and BaP was weakened, resulting in the blockage of their binding [16]. When the pH value was greater than 7.4, the removal of BaP by chromatin decreased. The reason for this phenomenon may be the increase in the amount of OH- in the solution, which led to the protonation of the relevant groups in the chromatin and inhibited the adsorption process [25]. Therefore, in this experiment, the optimum condition for the reaction was chosen to be pH 7.4. pH of solution changes the distribution of charge on the adsorbent surface, which in turn affects the adsorption performance of the adsorbent. When chromatin was used as an adsorbent for the treatment of BaP, the DNA was positively charged in the acidic solution and negatively charged in the basic solution [14]. The DNA in the chromatin is the active ingredient of the adsorbent, so changing the pH of the solution will have an effect on the adsorption.

3.6. The effect of chromatin quality on the removal efficiency of BaP

As showed in Fig. 3d, for the two concentrations of BaP solution, 100 $\mu g \cdot L^{-1}$, 200 $\mu g \cdot L^{-1}$, it could be found that the removal of BaP from the solution changed less with the increase of the amount of chromatin, and for the BaP solution of 300 $\mu g \cdot L^{-1}$, the removal rate showed an increasing trend with the increase of chromatin quality. When the chromatin quality was greater than 1.5 g L^{-1}, its BaP removal rate does not change significantly. When the chromatin dose is 1.5 g L^{-1}, for the 100 $\mu g \cdot L^{-1}$, 200 $\mu g \cdot L^{-1}$, 300 $\mu g \cdot L^{-1}$ BaP solutions, the BaP removal rates were 97 %, 91 %, and 68 %, respectively, and the BaP adsorption capacity of chromatin was 0.136 mg g^{-1}, indicating that BaP in the solution with lower BaP concentration has been almost completely removed. Under the same dosage of chromatin, as the concentration of BaP to be treated increases, the BaP removal rate of chromatin decreases. This may be due to the limited number of adsorption sites of the adsorbent itself, which have already been fully adsorbed. As the dosage of adsorbent increases, the number of adsorption sites also increases. Therefore, as the dosage of adsorbent increases, the BaP removal rate of

chromatin gradually improves. In order to ensure a higher removal rate without wasting the adsorbent, an adsorbent dosage of 1.5 g L^{-1} was selected as the optimal adsorbent quality.

3.7. The effect of initial concentration of BaP solution on the efficiency of chromatin removal

As showed in Fig. 3e, the BaP removal rate of chromatin gradually decreased with the increase of concentration of BaP solution. When the starting concentration of the BaP solution was low, the BaP removal rate was high, and when the BaP concentration increased from 100 μg·L^{-1} to 300 μg·L^{-1}, the BaP removal rate decreased sharply from 97 % to 79 %, however, the adsorption amount increased gradually from 0.064 mg g^{-1} to 0.158 mg g^{-1}. The reason for this phenomenon may be that the amount of chromatin is certain, and the number of adsorption sites available is limited, when the concentration of BaP solution is low, there are enough adsorption sites in the chromatin to adsorb BaP sufficiently, which is manifested as a high adsorption rate. As the BaP concentration of the solution increases, the number of adsorption sites in the original adsorbent remains unchanged, but the number of BaP molecules in the solution increases, resulting in insufficient adsorption and a lower removal rate.

3.8. Effect of environmental coexisting substances on BaP adsorption of chromatin

When the BaP concentration was 300 μg·L^{-1}, chromatin was1.5 g L^{-1}, the temperature of the reaction was 35 °C and the pH of the BaP solution was 7.4, the shaker reaction was carried out for 140 min, and the BaP removal rate of chromatin was only 79 %. This meant that at such a high BaP concentrations, although the BaP removal rate of chromatin was only 79 %, it was already the limit of chromatin's ability to remove BaP. Therefore, Therefore, to study the influence of environmental co-existing substances on the BaP removal efficiency by chromatin, glucose, lysine, vitamin C or leucine were added to the above removing BaP reaction by chromatin with concentrations as follow:1 × 10^{-2} mol L^{-1}, 2 × 10^{-3} mol L^{-1}, 4 × 10^{-4} mol L^{-1}, 8 × 10^{-5} mol L^{-1}, 1.6 × 10^{-5} mol L^{-1}, 3.2 × 10^{-6} mol L^{-1}, 6.4 × 10^{-7} mol L^{-1}. Urea was also added to the above removing BaP reaction by chromatin with concentrations as follow: 1 mol L^{-1}, 0.5 mol L^{-1}, 0.1 mol L^{-1}, 0.01 mol L^{-1}, 0.001 mol L^{-1}, 0.0001 mol L^{-1}. After the shaker reaction was carried out for 140 min, the results of their BaP removal rates were shown in Fig. 4. As shown in Fig. 4, it can be observed that the BaP removal rate of chromatin changes after adding several environmental coexisting substance such as lysine, leucine, glucose, vitamin C, or urea. The presence of lysine and vitamin C improved BaP removal rate of the adsorbent, increasing the removal rate by chromatin from 79 % to approximately 85 % compared to the absence of environmental coexisting substances. The presence of glucose and leucine decreased the removal of BaP from chromatin from 79 % to approximately 75 % compared to the absence of environmental coexisting substances.

For vitamins, the reason for this may be due to the fact that the oxidizing properties of vitamin C cause the DNA double helix structure in the stain to stretch more, favoring the intercalation of the BaP molecules into the base pairs of DNA [26]. For glucose, the reason for the decrease in the BaP removal rate may be due to the increase in the viscosity of the solution, which is unfavorable for molecular movement, and the chance of molecules contacting each other decreases, thus causing a decrease in the BaP removal rate [27]. For lysine, the reason for the increase in the removal rate may be due to the fact that lysine is a polar amino acid, and the polar carboxyl group in the amino acid will combine with the grooves of the DNA in the staining by hydrogen bonding, so that the original double helix structure of the DNA becomes loose, which is conducive to the intercalation between BaP molecules and DNA, and therefore the removal rate is increased by a small margin [28]. The main reason for the decrease in the BaP removal rate after the addition of a higher concentration of leucine is that leucine is a non-polar hydrophobic amino acid, and the hydrophobic groups on its side chain will bind to DNA and cause damage to DNA, which in turn affects the BaP removal rate of chromatin. However, a lower concentration of leucine can promote the interaction between DNA and BaP molecules in chromatin, which has a certain effect on improving the BaP removal rate [29].

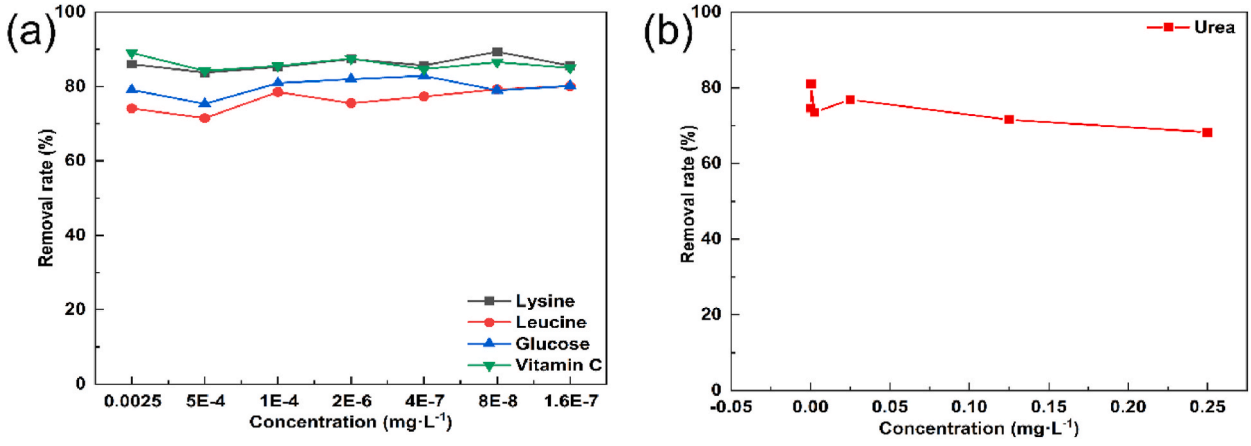

Fig. 4. (a) Effect of the presence of glucose, lysine, vitamin C, and leucine on the removal of BaP by chromatin. (b) Effect on chromatin removal of BaP in the presence of urea.

As can be seen from Fig. 4b, there is an influence of the presence of the environmental coexisting substance urea on the chromatin removal efficiency. The BaP removal rate of chromatin is gradually decreased with the gradual increase of urea concentration in the system. The reason for this phenomenon may be that the high urea concentration reduces the stability and rigidity of the double helix of DNA, so that the intercalating bite of BaP to the chromatin is blocked, resulting in a gradual decrease in the BaP removal rate as the concentration of urea gradually increases [30]. Environmental coexisting substances do have an impact on the BaP removal rate of chromatin. Some are beneficial for chromatin to remove BaP, while others are not.

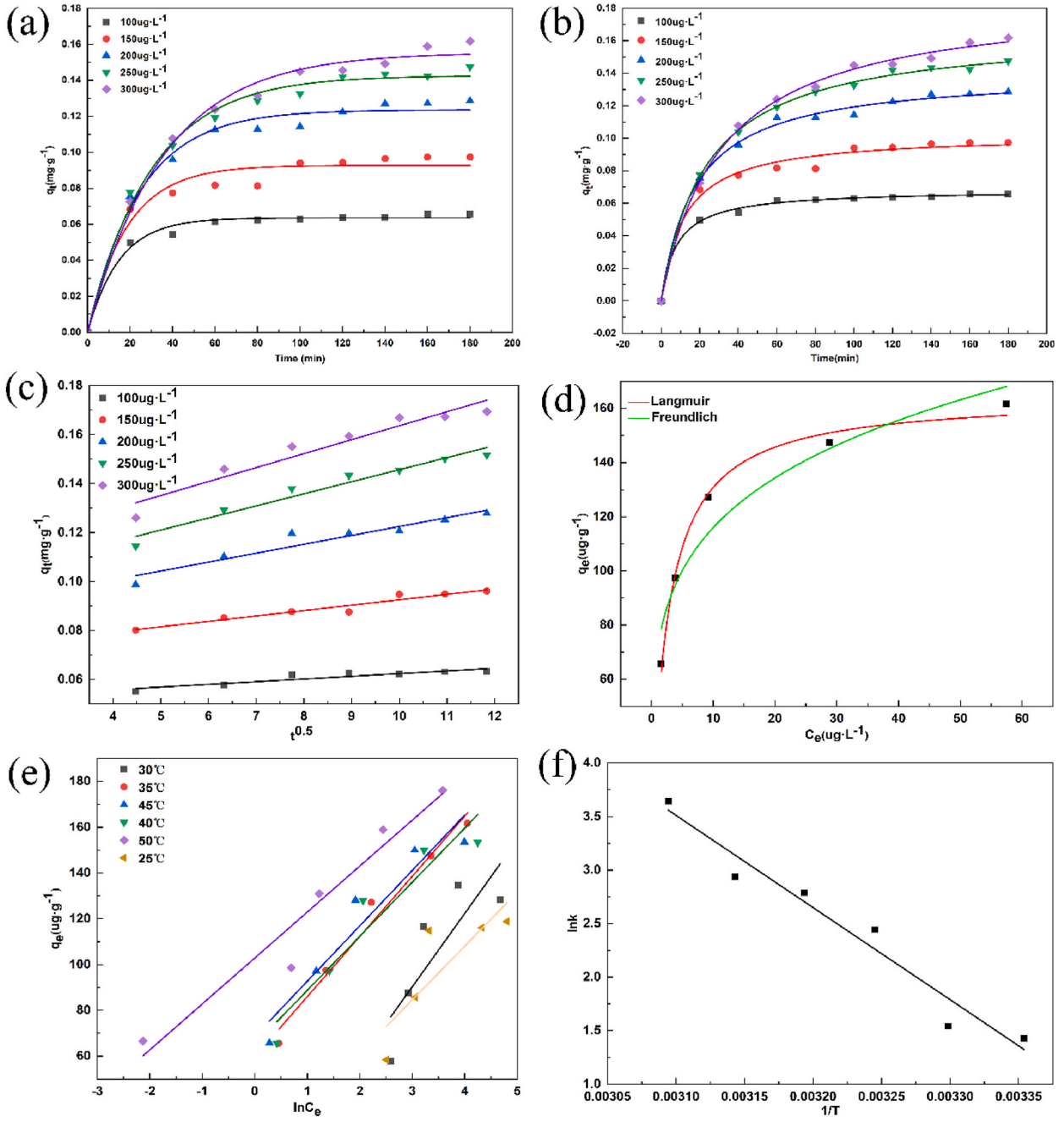

Fig. 5. (a) Chromatin adsorption BaP nonlinear first-order kinetic model plot. (b) Chromatin adsorption BaP nonlinear second-order kinetic model diagram. (c) Chromatin adsorption BaP intra-particle diffusion model. (d) Chromatin adsorption BaP Langmuir nonlinear isotherm and Freundlich nonlinear isotherm model plots. (e) Chromatin adsorption BaP Tekmin adsorption isotherm model plot. (f) Chromatin adsorption BaP adsorption thermodynamic diagram.

3.9. Adsorption kinetics

A detailed and accurate description of the processes and mechanisms involved in adsorption reactions is very important. Here we have used the nonlinear pseudo-first-order adsorption kinetic equation (1) and the nonlinear pseudo-second-order adsorption kinetic equation (2) for the relevant fitting illustrations [14].

$$q_t = q_e\left(1\text{-}exp^{\text{-}k_1 t}\right) \tag{1}$$

$$q_t = \frac{k_2 q_e{}^2 t}{1 + k_2 q_e t} \tag{2}$$

where t (min) represents the adsorption time and q_t ($mg{\cdot}g^{-1}$) corresponds to the amount of BaP adsorbed per unit mass of the chromatin when the adsorption time is t. q_e ($mg{\cdot}g^{-1}$) represents the amount of BaP adsorbed per unit mass of chromatin at adsorption equilibrium. Furthermore, k_1 $(min)^{-1}$ is the rate constant of the pseudo-first-order model, while k_2 $[g{\cdot}(mg{\cdot}min)^{-1}]$ is that of the pseudo-second-order model.

The fitted plots of the nonlinear adsorption kinetic model of BaP by chromatin are shown in Fig. 5a and b, respectively. The parameters resulting from the linear fits are provided in Table 1. From the comparison of the two values of correlation coefficient (R^2) and q_e in Tables 1 and it can be seen that the adsorption process of BaP by chromatin is more in line with the pseudo-second-order adsorption kinetic model [14].

Considering the possible influence of pores and intra-particle diffusion in the adsorption process, the analytical fitting was performed using equation (3). q_t is the adsorbed amount and t is the time [31].

$$q_t = k_3 t^{0.5} + C \tag{3}$$

k_3 ($mg{\cdot}g^{-1}{\cdot}min^{-0.5}$) represents velocity constants for the intraparticle diffusion model, and C is a constant.

The intraparticle diffusion model is able to show multiple stages involved in the adsorption process, including an initial surface adsorption stage, an asymptotic particle diffusion adsorption stage, and a final equilibrium stage. As shown in Fig. 5c and Table 1, the fitted lines for q_t and $t^{0.5}$ do not pass through the origin with a correlation coefficient of 0.81673–0.94597. This correlation coefficient suggests that intra-particle diffusion is not the only speed-limiting step. If it is the only rate-limiting step, then the line fitted by the intra-particle diffusion model should pass through the origin. In addition, it can be seen from the figure that the adsorption process of chromatin on BaP involves multiple steps, and surface adsorption and internal diffusion may occur simultaneously during the adsorption process.

3.10. Adsorption isotherm model

Chromatin adsorption isotherm models for BaP were fitted and analyzed using Langmuir (4) and Freundlich (5) adsorption isotherm model equations [14].

$$q_e = \frac{q_m k_L c_e}{1 + k_l c_e} \tag{4}$$

q_e: adsorbed amount at equilibrium; q_m: adsorbed amount at saturation; Ce: concentration of BaP at equilibrium; K_L: Langmuir's constant, as shown in Fig. 5d($R^2 > 0.99$).

$$q_e = k_F c_e^{\frac{1}{n}} \tag{5}$$

K_F: Freundlich constant, n: adsorption intensity, as shown in Fig. 5d($R^2 > 0.9$).

The Langmuir isotherm model indicates that the active sites of the adsorbent are uniformly distributed and uniformly adsorbed on the surface.The Freundlich isotherm model is mostly used to represent multilayer adsorption. The relevant parameters of both models are presented in Table 2. Notably, by comparing the correlation coefficients of the two models, it was concluded that the adsorption

Table 1
The data related to chromatin adsorption BaP adsorption kinetics.

BaP ($ug{\cdot}L^{-1}$)	Pseudo first-order dynamics			Pseudo second order dynamics			Intraparticle diffusion		
	K_1 (min^{-1})	q_e ($mg{\cdot}g^{-1}$)	R^2	K_2 ($g{\cdot}mg^{-1}{\cdot}min^{-1}$)	q_e ($mg{\cdot}g^{-1}$)	R^2	K_3 ($mg{\cdot}g^{-1}{\cdot}min^{-0.5}$)	C	R^2
100	0.019	0.019	0.901	1.93	0.068	0.999	0.0011	0.051	0.818
150	0.023	0.057	0.879	0.620	0.105	0.988	0.0022	0.070	0.926
200	0.025	0.097	0.856	0.390	0.141	0.995	0.0036	0.086	0.897
250	0.024	0.125	0.973	0.240	0.169	0.999	0.0049	0.096	0.946
300	0.018	0.109	0.966	0.190	0.181	0.998	0.0057	0.107	0.912

Table 2
Chromatin adsorption BaP Adsorption isotherm correlation data under linear fitting.

Isotherm model			Model parameter		
Langmuir	T (K)	K_L (L·mg^{-1})	q_m (mg·g^{-1})		R^2
	298.15	100	0.130		0.989
	303.15	85.0	0.146		0.963
	308.15	442	0.147		0.995
	313.15	500	0.158		0.999
	318.15	443	0.171		0.999
	323.15	874	0.181		0.998
Freundlich	T (K)	n	K_F (mg$^{1\text{-}1/n}$·L$^{1/n}$·g^{-1})		R^2
	298.15	3.73	0.231		0.570
	303.15	2.93	0.326		0.533
	308.15	5.04	0.265		0.428
	313.15	4.54	0.315		0.814
	318.15	4.16	0.369		0.867
	323.15	5.57	0.334		0.950
Dubinin-Radushkevich	T (K)	K_{ad} (mol^2·kJ)$^{-2}$	q_s (mg·g^{-1})	R^2	E (kJ·mol^{-1})
	298.15	-3.4×10^{-8}	0.342	0.998	3.8
	303.15	-3.3×10^{-8}	0.354	0.997	
	308.15	-3.4×10^{-8}	0.377	0.996	
	313.15	-3.3×10^{-8}	0.385	0.996	
	318.15	-3.3×10^{-8}	0.392	0.995	
	323.15	-3.2×10^{-8}	0.403	0.994	
Temkin	T (K)	K_T	B(kJ·mol^{-1})	R^2	
	298.15	1.808	23.540		0.611
	303.15	0.831	32.070		0.590
	308.15	9.628	26.322		0.968
	313.15	15.619	23.654		0.877
	318.15	16.904	24.216		0.890
	323.15	167.521	20.081		0.927

process of BaP by chromatin is more consistent with the Freundlich adsorption isotherm model. The Freundlich isotherm model better elucidates the interaction between BaP and the chromatin, suggesting the multilayer adsorption of BaP with the composite and heterogeneity on the surface of the chromatin. The value of n > 1 implies a favorable and strong interaction between BaP and the chromatin, signifying favorable BaP adsorption.

The Dubinin-Radushkevich model (6) is used to describe the energy of the adsorbent molecules and is abbreviated as E, which represents the energy required for the movement of the molecules.E < 8 kJ mol^{-1}, indicates that the adsorption process is physisorption.8 kJ mol^{-1}<E < 16 kJ mol^{-1}, indicates that the adsorption process is chemisorption [16].

$$ln\ q_e = ln\ q_s\text{-}k_{ad}\varepsilon^2 \tag{6}$$

where K_{ad}[(mol^2·kJ)$^{-2}$] represents the Dubinin-Radushkevich isothermal modelling constants, q_s (mg·g^{-1}) iscorresponds to the theoretical saturation capacity of isothermal models, and ε (mol^2·kJ^{-2}) refers to the Polanyi potential as defined by Eq. (7), while E (kJ·mol^{-1}) can be calculated using Eq. (8) [16].

$$\varepsilon = RTln\left(1+\frac{1}{C_e}\right) \tag{7}$$

$$E = \frac{1}{\sqrt{\text{-}2k_{ad}}} \tag{8}$$

Based on the linear fitting results presented in Table 2, E was determined to be 3.8 kJ mol^{-1}. Since E is below 8 kJ mol^{-1}, the adsorption process could be judged to be a physisorption process. Consequently, the adsorption of BaP by the chromatin is attributed to physisorption process.

The Temkin isotherm model incorporates an explicit consideration of adsorbent-adsorbate interactions. As shown in equation (9) used, this equation results in a uniform distribution of the binding energy [32,33].

$$q_e = BlnK_T + BlnC_e \tag{9}$$

K_T is the equilibrium constant and B(kJ·mol^{-1}) is the adsorption energy. The data associated with the modified isotherm model fit are shown in Table 2. The Temkin model fit as shown in Fig. 5e. The adsorption energy of the adsorbent is all positive, and the adsorption process is a heat-absorbing process.

To gain further insights into the thermodynamic characteristics of BaP adsorption on the chromatin, experiments were conducted at different temperatures. The Gibbs radical change (ΔG), the standard change in entropy (ΔS) and the standard change in enthalpy (ΔH) are computed using Eq$_s$. (10)-(12).

$$\Delta G = \text{-RTln } K_L \tag{10}$$

$$ln\, K_L = \frac{\Delta S}{R} - \frac{\Delta H}{RT} \tag{11}$$

$$\Delta G = \Delta H\text{-}T\Delta S \tag{12}$$

where ΔG represents the Gibbs free energy (kJ·mol^{-1}), R denotes the gas constant (8.314 J mol^{-1} K^{-1}), K_L represents the thermodynamic equilibrium constant of adsorption, and ΔH represents the enthalpy change of adsorption (kJ). Adsorption thermodynamics related data in Table 3. The adsorption thermodynamic fit is shown in Fig. 5f.

4. Conclusion

In this study, a series of adsorption experiments and related detection techniques were used to verify the feasibility of chromatin prepared from carp spermathecae as a viable potential adsorbent for BaP. The results of Fourier infrared spectroscopy showed that proteins and DNA were present in the chromatin, and a good binding between chromatin and BaP was formed. Observations by scanning electron microscopy and fluorescence microscopy showed that chromatin had a good adsorption effect on BaP. The results of batch adsorption experiments showed that the chromatin reached adsorption equilibrium for each concentration of BaP for 140 min under the conditions of pH 7.4 and temperature 35 °C, and the BaP removal was completed. In addition, the adsorption kinetic fitting results showed that the adsorption of BaP by chromatin conformed to the pseudo-second-order kinetic model. The results of adsorption isotherm fitting showed that the adsorption process was more in line with the Langmuir isotherm model, and the adsorption capacity of chromatin on BaP was 0.16 mg g^{-1}. The results of Dubinin-Radushkevich isotherm fitting showed that the adsorption of BaP by chromatin was a physical adsorption process. The results of the Tekmin adsorption isotherm study indicate that the adsorption process is heat-absorbing and the thermodynamic results indicate that the adsorption process is spontaneous. In summary, the chromatin extracted from the testis of common carp has good performance in removing BaP and can be used as a novel feasible adsorbent for efficient removal of BaP from pollutants.

Data availability

The relevant data for this study are not deposited in the relevant repository and will be covered in further relevant subsequent studies.Data will be made available on request.

Funding

This work was supported by the National Natural Science Foundation of China (Grant numbers 22265003 and 21966008).

Ethical approval

Not applicable.

Consent to participate

Not applicable.

Consent to publication

The authors have consented to the submission of the study to the journal.

Ethics declarations

Informed consent was not required for this study because the data used in this study were experimentally obtained and authentic.

Table 3
Chromatin adsorption BaP adsorption thermodynamic correlation data.

T(K)	ΔG (kJ·mol^{-1})	ΔH (kJ·mol^{-1})	ΔS (J·mol^{-1}·K^{-1})
298.15	−3.53		
303.15	−3.88		
308.15	−6.26	71.55	252.5
313.15	−7.26		
318.15	−7.77		
323.15	−9.79		

Description of data analysis

All the data in this study were analyzed by origin2021 software.

CRediT authorship contribution statement

Zhikang Jiang: Writing – review & editing, Writing – original draft, Visualization, Validation, Software, Resources, Project administration, Methodology, Investigation, Formal analysis, Data curation, Conceptualization. **Junsheng Li:** Writing – review & editing, Supervision, Funding acquisition, Conceptualization. **Guoxia Huang:** Supervision. **Liujuan Yan:** Supervision. **Ji Ma:** Supervision.

Declaration of competing interest

The authors declare the following financial interests/personal relationships which may be considered as potential competing interests:Junsheng Li reports financial support, article publishing charges, and equipment, drugs, or supplies were provided by National Natural Science Foundation of China. If there are other authors, they declare that they have no known competing financial interests or personal relationships that could have appeared to influence the work reported in this paper.

Acknowledgments

We gratefully acknowledge the support and funding from the National Natural Science Foundation of China. We thank Guangxi University of Science and Technology and Guangxi Key Laboratory of Green Processing of Sugar Resources for their support.

References

[1] A. Sakshi, Haritash. A comprehensive review of metabolic and genomic aspects of PAH-degradation, Arch. Microbiol. 202 (2020) 2033–2058, https://doi.org/10.1007/s00203-020-01929-5.
[2] H. Shen, S. Grist, D. Nugegoda, The PAH body burdens and biomarkers of wild mussels in Port Phillip Bay, Australia and their food safety implications, Environ. Res. 188 (2020) 109827, https://doi.org/10.1016/j.envres.2020.109827.
[3] M. Wu, X. Guo, J. Wu, K. Chen, Effect of compost amendment and bioaugmentation on PAH degradation and microbial community shifting in petroleum-contaminated soil, Chemosphere 256 (2020) 126998, https://doi.org/10.1016/j.chemosphere.2020.126998.
[4] Y. Xiong, J. Li, G. Huang, L. Yan, J. Ma, Interacting mechanism of benzo(a)pyrene with free DNA in vitro, Int. J. Biol. Macromol. 167 (2021) 854–861, https://doi.org/10.1016/j.ijbiomac.2020.11.042.
[5] F. Chapman, C. Sparham, C. Hastie, D. Sanders, R. Egmond, K. Chapman, S. Doak, A. Scott, G. Jenkins, Comparison of passive-dosed and solvent spiked exposures of pro-carcinogen, benzo[a]pyrene, to human lymphoblastoid cell line, MCL-5, Toxicol. Vitro 67 (2020) 104905, https://doi.org/10.1016/j.tiv.2020.104905.
[6] Q. Gu, C. Hu, Q. Chen, Y. Xia, J. Feng, H. Yang, Development of a rat model by 3,4-benzopyrene intra-pulmonary injection and evaluation of the effect of green tea drinking on p53 and bcl-2 expression in lung carcinoma, Cancer Detect. Prev. 32 (2009) 444–451, https://doi.org/10.1016/j.canep.2009.04.002.
[7] J. Chen, S. Chen, Removal of polycyclic aromatic hydrocarbons by low density polyethylene from liquid model and roasted meat, Food Chem. 90 (2005) 461–469, https://doi.org/10.1016/j.foodchem.2004.05.010.
[8] C. Yuan, A. Davis, D. Kaya, B. Kjellerup, Distribution and biodegradation potential of polycyclic aromatic hydrocarbons (PAHs) accumulated in media of a stormwater bioretention, Chemosphere 336 (2023) 139188, https://doi.org/10.1016/j.chemosphere.2023.139188.
[9] E. Torres, I. Bustos-Jaimes, S. Le Borgne, Potential use of oxidative enzymes for the detoxification of organic pollutants, Appl. Catal. B Environ. 46 (2003) 1–15, https://doi.org/10.1016/S0926-3373(03)00228-5.
[10] E. Psillakis, G. Goula, N. Kalogerakis, D. Mantzavinos, Degradation of polycyclic aromatic hydrocarbons in aqueous solutions by ultrasonic irradiation, J. Hazard Mater. 108 (2004) 95–102, https://doi.org/10.1016/j.jhazmat.2004.01.004.
[11] B. Bogan, V. Trbovic, J. Paterek, Inclusion of vegetable oils in FentonÕs chemistry for remediation of PAH-contaminated soils, Chemosphere 50 (2003) 15–21, https://doi.org/10.1016/s0045-6535(02)00490-3.
[12] D. Mahringer, S. Zerelli, U. Dippon-Deißler, A. Ruhl, Biogenic amorphous ferric hydroxide as adsorbent for vanadium removal in drinking water production, Environ. Technol. Innovat. 32 (2023) 103239, https://doi.org/10.1016/j.eti.2023.103239.
[13] G. Panigrahi, N. Verma, N. Singh, S. Asthana, S. Gupta, A. Tripathi, M. Das, Interaction of anthraquinones of Cassia occidentalis seeds with DNA and Glutathione, Toxicol Rep 5 (2018) 164–172, https://doi.org/10.1016/j.toxrep.2017.12.024.
[14] G. Huang, J. Li, L. Yan, J. Ma, Adsorption of 1, 2-benzanthracene from aqueous solution by DNA-conjugated magnetic nanoparticles, Water Air Soil Pollut. 233 (2022) 9, https://doi.org/10.1007/s11270-021-05476-7.
[15] G. Huang, J. Ma, J. Li, L. Yan, Removal of 1,2-benzanthracene via the intercalation of 1,2-benzanthracene with DNA and magnetic bead-based separation, Nucleos Nucleot. Nucleic Acids (2020) 1–20, https://doi.org/10.1080/15257770.2020.1839905.
[16] J. Zhang, J. Li, G. Huang, L. Yan, Chromatin extracted from common carp testis as an economical and easily available adsorbent for ethidium bromide decontamination, Heliyon 8 (2022) e09565, https://doi.org/10.1016/j.heliyon.2022.e09565.
[17] M. Artman, J. Roth, Chromosomal RNA: an artifact of preparation? J. Mol. Biol. 60 (1971) 291–301, https://doi.org/10.1016/0022-2836(71)90295-6.
[18] D. Jangir, S. Charak, R. Mehrotra, S. Kundu, FTIR and circular dichroism spectroscopic study of interaction of 5-fluorouracil with DNA, J. Photochem. Photobiol. B Biol. 105 (2011) 143–148, https://doi.org/10.1016/j.jphotobiol.2011.08.003.
[19] D. Jangir, G. Tyagi, R. Mehrotra, S. Kundu, Carboplatin interaction with calf-thymus DNA: a FTIR spectroscopic approach, J. Mol. Struct. 969 (2010) 126–129, https://doi.org/10.1016/j.molstruc.2010.01.052.
[20] S. Saito, G. Silva, C. Pungartnik, M. Brendel, Study of DNA-emodin interaction by FTIR and UV-vis spectroscopy, J. Photochem. Photobiol. B Biol. 111 (2012) 59–63, https://doi.org/10.1016/j.jphotobiol.2012.03.012.
[21] Z. Cui, Z. Zheng, L. Lin, J. Si, Q. Wang, X. Peng, W. Chen, Electrospinning and crosslinking of polyvinyl alcohol/chitosan composite nanofiber for transdermal drug delivery, Adv. Polym. Technol. 37 (2018) 1917–1928, https://doi.org/10.1002/adv.21850.
[22] K. Onchoke, C. Hadad, P. Dutta, Structure and vibrational spectra of mononitrated benzo [a]pyrenes, J Phys Chem A. 110 (2006) 76–84, https://doi.org/10.1021/jp054881d.
[23] D. Staynov, Thermal denaturation profiles and the structure of chromatin, Nature 264 (1976) 522–525, https://doi.org/10.1038/264522a0.
[24] P. Pantazis, M. Sakamoto, Thermostability of chromatin and variations in chromosomal proteins isolated under different ionic conditions, J. Biochem. 88 (1980) 1283–1289, https://doi.org/10.1093/oxfordjournals.jbchem.a133097.

[25] H. Qi, N. Bi, Y. Chen, X. Zheng, H. Zhang, Y. Chen, Y. Tian, A DNA biosensor based on resonance light scattering using unmodified gold bipyramids, Microchim. Acta 178 (2012) 131–137, https://doi.org/10.1007/s00604-012-0823-4.
[26] P. Chanphai, H. Tajmir-Riahi, Vitamin C binding efficacy with DNA and RNA, J. Mol. Liq. 286 (2019) 110925, https://doi.org/10.1016/j.molliq.2019.110925.
[27] R. Juan, Role of Co-solute in biomolecular stability: glucose, urea and the water structure, J. Biol. Phys. 27 (2001) 73–79, https://doi.org/10.1023/A:1011890506834.
[28] C. Li, J. Li, G. Huang, Q. Li, L. Yan, Assessment of potential toxicity of Alizarin through resonance light scattering, Asian J. Chem. 25 (2013) 1015–1020, https://doi.org/10.14233/ajchem.2013.13365.
[29] R. da Luz Dias, B. Basso, M. Donadio, F. Pujol, R. Bartrons, G. Haute, R. Gassen, H. Bregolin, G. Krause, C. Viau, J. Saffi, F. Nunes, J. Rosa, J. de Oliveira, Leucine reduces the proliferation of MC3T3-E1 cells through DNA damage and cell senescence, Toxicol. Vitro 48 (2017) 1–10, https://doi.org/10.1016/j.tiv.2017.12.015.
[30] C. Zhu, J. Li, Optical Tweezers analysis of double-stranded DNA denaturation in the presence of urea, J. Phys. Soc. Jpn. 85 (2016) 094004, https://doi.org/10.7566/JPSJ.85.094004.
[31] M. Rajabi, O. Moradi, K. Zare, Kinetics adsorption study of the ethidium bromide by graphene oxide as adsorbent from aqueous matrices, Int. Nano Lett. 7 (2017) 35–41, https://doi.org/10.1007/s40089-017-0199-x.
[32] A. Khatibi, M. Yilmaz, A. Mahvi, D. Balarak, S. Salehi, Evaluation of surfactant-modified bentonite for Acid Red 88 dye adsorption in batch mode: kinetic, equilibrium, and thermodynamic studies, Desalination Water Treat. 271 (2022) 48–57, https://doi.org/10.5004/dwt.2022.28812.
[33] F. Mostafapour, A. Mahvi, A. Khatibi, M. Saloot, N. Mohammadzadeh, D. Balarak, Adsorption of lead(II) using bioadsorbent prepared from immobilized Gracilaria corticata algae: thermodynamics, kinetics and isotherm analysis, Desalination Water Treat. 265 (2022) 103–113, https://doi.org/10.5004/dwt.2022.28627.